REPORT DOCUMENTATION PAGE

Form Approved
OMB No. 0704-0188

1. REPORT DATE *(DD-MM-YYYY)*	**2. REPORT TYPE**	**3. DATES COVERED** *(From - To)*
31-03-2008	Technical Paper	

4. TITLE AND SUBTITLE

Effects of a Variable-Phase Transverse Acoustic Field on a Coaxial Injector at Subcritical and Near-Critical Conditions (Preprint)

5a. CONTRACT NUMBER

5b. GRANT NUMBER

5c. PROGRAM ELEMENT NUMBER

6. AUTHOR(S)
Juan I. Rodriguez, Ivett A. Leyva, & Douglas Talley (AFRL/RZSA); Bruce Chehroudi (ERC)

5d. PROJECT NUMBER

5e. TASK NUMBER
23080533

5f. WORK UNIT NUMBER

7. PERFORMING ORGANIZATION NAME(S) AND ADDRESS(ES)

Air Force Research Laboratory (AFMC)
AFRL/RZSA
10 E. Saturn Blvd.
Edwards AFB CA 93524-7680

8. PERFORMING ORGANIZATION REPORT NUMBER

AFRL-RZ-ED-TP-2008-081

9. SPONSORING / MONITORING AGENCY NAME(S) AND ADDRESS(ES)

Air Force Research Laboratory (AFMC)
AFRL/RZS
5 Pollux Drive
Edwards AFB CA 93524-7048

10. SPONSOR/MONITOR'S ACRONYM(S)

11. SPONSOR/MONITOR'S NUMBER(S)
AFRL-RZ-ED-TP-2008-081

12. DISTRIBUTION / AVAILABILITY STATEMENT

Approved for public release; distribution unlimited (PA #08117A).

13. SUPPLEMENTARY NOTES
Submitted for presentation at the 21st ILASS-Americas Meeting, Orlando, FL, 18-21 May 2008.

14. ABSTRACT

An experimental study that focuses on the effects of a variable transverse acoustic field on an N_2 shear coaxial jet is presented. The coaxial jet is exposed to different acoustic conditions by varying the phase between two acoustic sources. The main objective of this investigation is to analyze the effect of transverse acoustic forcing with variable phase on the magnitude of the inner-jet dark-core length. The coaxial jet is exposed to a subcritical and near-critical pressure environment. The measurements are performed on backlit images of the coaxial jet obtained with a high-speed camera. The momentum flux ratio of the outer to the inner jet is varied from 1 to 20 for subcritical conditions and from 0.6 to 5 for near-critical conditions. The resonant frequency of the system is approximately 3 kHz and the maximum pressure variation with respect to total pressure is 3%. It is found that at subcritical pressures the effects of these variable acoustic fields on the length of the dark core achieve a maximum for momentum flux ratios between 1 to 5.

15. SUBJECT TERMS

16. SECURITY CLASSIFICATION OF:			**17. LIMITATION OF ABSTRACT**	**18. NUMBER OF PAGES**	**19a. NAME OF RESPONSIBLE PERSON**
					Dr. Douglas Talley
a. REPORT	**b. ABSTRACT**	**c. THIS PAGE**	SAR	12	**19b. TELEPHONE NUMBER** *(include area code)*
Unclassified	**Unclassified**	**Unclassified**			N/A

Effects of a Variable-Phase Transverse Acoustic Field on a Coaxial Injector at Subcritical and Near-Critical Conditions (Preprint)

Juan I. Rodriguez*, Ivett A. Leyva, Bruce Chehroudi and Douglas Talley
Air Force Research Laboratory, Edwards AFB, CA 93524 USA

Abstract

An experimental study that focuses on the effects of a variable transverse acoustic field on an N_2 shear coaxial jet is presented. The coaxial jet is exposed to different acoustic conditions by varying the phase between two acoustic sources. The main objective of this investigation is to analyze the effect of transverse acoustic forcing with variable phase on the magnitude of the inner-jet dark-core length. The coaxial jet is exposed to a subcritical and near-critical pressure environment. The measurements are performed on backlit images of the coaxial jet obtained with a high-speed camera. The momentum flux ratio of the outer to the inner jet is varied from 1 to 20 for subcritical conditions and from 0.6 to 5 for near-critical conditions. The resonant frequency of the system is approximately 3 kHz and the maximum pressure variation with respect to total pressure is 3%. It is found that at subcritical pressures the effects of these variable acoustic fields on the length of the dark core achieve a maximum for momentum flux ratios between 1 to 5.

* Corresponding author

Introduction

Coaxial injectors such as those used for the J-2 engine and the Space Shuttle Main Engine are of fundamental importance in cryogenic liquid rocket engine (LRE) studies. Due to improvements experienced in performance of LRE's at high mean combustion chamber pressures, the critical value of some propellants has been reached and surpassed. Thus, incidents of high frequency combustion instabilities, potentially causing engine and vehicle damage or destruction, are of critical importance to understand under these pressures.

Of particular importance in combustion instability is the outer to inner jet velocity ratio. It was found that at high velocity ratios the combustion is more stable[1]. Another important parameter is the mean chamber pressure (p) of the combustion chamber. In recent studies, Marshall et al.[2] evaluated the influence of mass flow rate, mixture ratio, injector and nozzle positions and chamber pressure on the spontaneous excitation of transverse modes. Operating at 1.53 MPa, maximum amplitudes of 4% of the peak-to-peak pressure perturbation (Δp) as a fraction of p were observed. Richecoeur et al.[3] obtained strong coupling between the combustion products from three coaxial $CH_4/0_2$ injectors and an imposed transverse acoustic field reaching 7% $\Delta p/p$ with a mean chamber pressure of 0.9 MPa. They also observed that combustion is more sensitive to acoustics at low outer jet velocities.

In the present study, both $\Delta p/p$ and momentum flux ratio (MR) are considered to characterize and understand the effects of a variable-phase transverse acoustic field on non-reacting coaxial injectors at conditions below and near the critical pressure of the propellant. The effect of the magnitude and phase of the pressure oscillations on the jet is characterized in this study by examining the behavior of the dark-core length of the inner jet. In previous experiments, the position of the injector with respect to the acoustic field profile was fixed. Only one acoustic driver was used to generate a transverse field and a reflective wall was placed at the other end of the test section. With this configuration, Leyva et al.[4,5] reported that the effects of the externally imposed acoustic field on the dark core length are greatest at subcritical pressures and for MR's between 1 and 4. In the present paper, however, the addition of a second acoustic driver allowed changes of the relative position of the acoustic field with respect to the fixed location of the coaxial jet injector. Preliminary results with this new setup at subcritical pressures were presented in Leyva et al.[6] Consistent with previous studies[4,5], it was found that the maximum changes in the dark-core length for subcritical pressures were statistically significant for MR=2.6 but not for MR=1. The present study extends the range of the MR's studied for subcritical conditions and introduces results for the (higher) near-critical pressures. The amplitude of the pressure oscillations was maximized to obtain the highest fractional change of the chamber pressure, which was typically between 1 to 3%. The momentum flux ratio of the outer to the inner jet was varied from 1 to 20 for subcritical and from 0.6 to 5 for near-critical conditions.

Experimental Setup

The Cryogenic Supercritical Laboratory (EC-4) facilities of the Air Force Research Laboratory (AFRL) at Edwards Air Force Base, CA were used to perform the experiments. Figure 1 shows the main chamber and the supporting systems. In the current setup, ambient temperature N_2 is used to supply flow to the inner and outer jet and also to pressurize the chamber. To avoid the inherent difficulties in computing the critical lines for mixtures versus having a well characterized critical point for a single element, molecular nitrogen (N_2) was used as the working fluid. The critical temperature of N_2 is 126.2 K and its critical pressure is 3.39 MPa. The central jet of a coaxial jet design entered the combustion chamber at subcritical temperatures and the outer jet was introduced at supercritical temperatures. These conditions resemble typical applications of liquid rocket engine systems. For example, a LOX/LH2 engine features an O_2 center jet at subcritical temperatures and an H_2 outer jet at supercritical temperatures. H_2 is delivered at higher temperatures because it is used as a coolant for the engine nozzle. A typical velocity ratio between the outer and the inner jet is 10^7. The inner tube producing the inner jet has an inner diameter, D1, of 0.51 mm with length-to-inside-diameter ratio of 100 jet diameter. The inner tube exit plane is recessed by 0.3 mm from the outer tube. The outer annular jet's inner diameter, D2, is 1.59 mm with outer diameter, D3, of 2.42 mm. For the outer jet, the length-to-mean-width of the annular passage is 67. Both the inner and the outer jets are cooled by heat exchangers (HE's) using liquid nitrogen obtained from a cryogenic tank. One heat exchanger cools the inner jet and other two cool the outer jet. Depending on the setup, one of these HE's can be bypassed to modify the cooling patterns. The mass flow rates of liquid nitrogen through the HE's are regulated in order to control the temperature of the jets. These rates are measured with Porter® mass flow meters (122 and 123-DKASVDAA) at ambient conditions to avoid difficulties with mass flow rate measurement at cryogenic temperatures. Also, an inner chamber was built and housed inside the main chamber to maintain the amplitude of the acoustic oscillations to a maximum at the test section. The inner chamber is 6.6cm high, 7.6cm wide and 1.3cm deep (see Fig. 1). The coaxial injector is shown in Fig. 2.

The chamber pressure is measured with a Stellar 1500 transducer. An unshielded type E thermocouple with a bead diameter of 0.1mm is used to measure the temperature of the jets. The accuracy of this thermocouple was checked with an RTD and found to be ±1K. Also, a Kulite® XQC-062 pressure transducer is used to measure the pressure near the location of the thermocouple tip at a sampling frequency of 20 kHz (see bottom right picture in Fig. 1). Both the pressure transducer and the thermocouple are moved in the plane perpendicular to the jet axis with two linear positioning stages built by Atto**cube** Systems AG. Each stage has a range of about 3 mm in 1 dimension with step sizes in the order of 0.01mm. One stage was placed on top of the other with their axis of movement perpendicular to each other for a total maximum interrogation area of 3 mm by 3 mm. The thermocouple and pressure transducer were fixed to a custom made probe stand mounted on top of the positioning assembly. In turn, the linear stages were placed at the top end of a shaft that rested on a large 4-inch range linear stage built by SETCO™ outside the main chamber. Thus, the temperature probe approaches the coaxial jet from the bottom and it can get arbitrarily close to the exit plane. This thermocouple has even been used to measure the temperature within the recess of the inner jet. NIST's REFPROP© and its thermophysical properties online database[8,9], are used to obtain density, viscosity, and surface tension from the measured flow rates, chamber pressure and jet temperature. From these properties, Re, We, outer to inner jet velocity ratio (VR) and MR for a given condition are then calculated.

The imaging of the coaxial flow was accomplished using a Phantom® 7.1 CMOS camera. The camera can be seen facing the main chamber in the bottom left picture of Figure 1. Backlit images with a resolution of 128x224, 128x256 or 128x304 pixels were obtained, with each pixel representing an area of approximately 0.08 mm by 0.08 mm. The framing rate was 20-25 kHz. The exposure time generally was 1-2 μs and the number of images saved per run was 1000 on average. The jet was backlit using a Newport® variable power arc lamp set at 160W. The dark core lengths are measured from 998 images using a MATLAB® subroutine based on the Otsu technique[10] to find a grayscale threshold which helps identify the inner core from the rest of the image (see Fig. 3). Two piezo-sirens custom-designed by Hersh Acoustical Engineering, Inc. were used to generate the transverse acoustic field (see Fig. 1). The principle by which the piezo-sirens work as acoustic drivers is relatively simple, with a piezo element moving an aluminum cone attached to it, which in turn produces acoustics waves. When the two drivers have a zero degree phase angle difference then the movement of the piezo-siren cones is synchronized and they move in opposite directions, that is, towards and away from each other simultaneously. On the contrary, when the two drivers have a 180-degree phase difference, then the cones move in the same direction. This behavior is represented by the sketches in Fig. 4. A Fluke® signal generator was used to drive the piezo-ceramic element of each piezo-siren with a sinusoidal wave at the preferred driving frequency of the system. The frequency was manually varied using a signal generator until the highest amplitudes of the pressure waves were obtained. These frequencies spanned a range between 2.95 and 3.10 kHz. Then the signals were amplified and fed to the piezo-sirens. The phase between the two elements was modified through each case to expose the coaxial jet to different locations within the acoustic field. The voltage supplied to the two acoustic drivers was the same for all cases and the phase difference was controlled by changing the phase of one acoustic driver with respect to the other using a lead/follower configuration in the signal generator. A waveguide with a catenary contour was used to guide the waves from a circular cross-section at the end of the aluminum cone to the rectangular cross-section of the rectangular inner chamber.

Results and Discussion

The main parameters studied were the curved (or total) length and the axial length of the dark core region of the inner jet as the phase difference between the acoustic drivers was varied. These two parameters are defined due to the sinusoidal shape imposed by the acoustic field. The axial length is the projection of the dark core of the inner jet onto the jet centerline and the curved length is the distance along the curved shape of the core in order to take into account the curvature produced by the acoustic field (see Fig. 3). For a more detailed explanation of the definitions for the axial and curved dark core lengths and the techniques employed to measure them, refer to Leyva et al.[5] The present study includes the findings of 5 cases at subcritical pressures and 3 cases at near-critical pressures. The effects of the imposed acoustic field on one subcritical case (P = 1.51 MPa, MR = 4.2) and one near-critical case (P = 3.55 MPa, MR = 2) are reviewed in detail. The coaxial jet for these two cases is shown in Figs. 5 and 6. Each figure contains two images. The image to the left shows the jet without acoustic forcing ("jet baseline") while the image to the right shows the jet at the phase difference where maximum changes in length were measured when compared to the jet baseline. The effect of the acoustic field on the bending of the jet is clearly visible. The near-critical case definitely shows a more enhanced curvature compared to its baseline but it is not as strong as its subcritical counterpart.

Figs. 7 to 10 show the axial and curved dark core lengths normalized by the inner jet diameter plotted

against the various phase differences between acoustic drivers for the cases pictured in Figs. 5 and 6. A secondary axis includes the measured Δp/p at each phase difference. The dark core length in the absence of the acoustic field (both drivers off) is considered as the reference baseline and also shown. For a few phase angles, the dark core length for when only one driver is acting is also indicated. The error bars shown represent ± 1σ of the lengths recorded for a given MR and phase angle difference. For the subcritical case, a statistical difference with respect to the baseline length can be observed for most phase angles. In contrast, for the near-critical condition the error bars at each phase angle are within the error bars of the baseline. Nonetheless, both conditions show a statistically-significant reduction of the dark core length under the acoustic field for at least one angle when both drivers are operating. As we would expect, the dark core length is longest when there are no acoustic disturbances. If there is only one source, the length decreases with respect to the baseline and this length is repeatable (within the error) for different angles, since the acoustic field created by that source remains the same at different phase angles if the other acoustic source is off.

Peak-to-peak pressure perturbations (Δp) generated in the inner chamber by the acoustic waves ranged from 10 to 35 kPa, which translated to different Δp/p conditions depending on the mean chamber pressure. In Fig. 7, there is a region where the axial dark core length is reduced to approximately 10D1 from a 15D1 baseline for phase angle differences between 0° and 135° until it starts increasing and it reaches a maximum between 270° and 315°. Interestingly, Δp/p has a maximum of 2.9% at 45° and a minimum of 1.5% at 225°. It is important to remember that the changes in Δp/p are entirely due to the phase angle since the driving voltage for the two sources is constant throughout the phase sweep experiment. It can be observed that for this case the minimum dark core length occurs at phase angles where there is a maximum in Δp/p, which corresponds to the pressure antinode of the acoustic field. In contrast, there is a region where the minimum dark core lengths coincide with the location of the pressure node or minimum Δp/p. These trends are the same observed for the curved dark core length as a function of phase angle difference in Fig 8.

In the near-critical range (Fig. 9), the difference between the baseline case and the minimum axial dark core length was 4D1 with a Δp/p range from 0.7% to 0.9% for these measurements. Even though the absolute acoustic field intensity is the same as the subcritical case, the higher near-critical pressure decreases the total relative intensity. Thus the difference between maximum and minimum values of the pressure perturbation is in fact near the minimum resolution of the pressure transducer. This increases the uncertainty of the measurements in the near-critical regime, making it difficult to quantify the effect of phase angle difference. Nevertheless, it can be seen that at least for one phase angle, the difference between the dark core length with and without acoustic forcing lies outside the error bars, which provides at least one data point where the difference between acoustics and no acoustics can be quantified.

Comparing the two cases that we have been studying in detail, the maximum difference in axial and curved dark core lengths was larger for the subcritical case compared to that of the near critical case by 55% and 28% respectively (see Figs. 7-10). These results show the greater impact the acoustic field had in the subcritical case compared to the near-critical case. This is to be expected due to the higher Δp/p attained for the subcritical case.

The difference between the baseline dark core length and the minimum dark core length achieved during the angle sweep normalized by the baseline value ("maximum length change/baseline length") for each of the 8 cases reported in this study is presented in Figs. 11 and 12. The difference in length is plotted as a function of MR. In the near-critical regime the three cases lie within a 30-40% with respect to the axial dark core baseline and within ~24-32% with respect to the curved dark core baseline. This could be indicative of a weak effect of the acoustics on the jet due to relatively low forcing or a particular trend within this MR range. More extensive studies in the near-critical regime would be needed to reach a definitive conclusion. However, for subcritical pressures, this difference was the largest at a range of momentum flux ratios between 1 and 5. The largest decrease in length of the dark core compared to the case with no acoustics was observed in this regime. These findings support previous experimental results that had shown similar behavior with one acoustic driver configuration[4,5] and preliminary data with two acoustic resonators[6].

Conclusions

The effects of an externally imposed transverse acoustic field with variable relative phase angle on the behavior of a shear coaxial jet are presented in this study. For the detailed analysis of one subcritical case at MR = 4.2 and one near-critical case at MR = 2, a statistically significant reduction of the inner jet dark core length with acoustic forcing was observed for most phase angles for the former case and at least one phase angle for the latter. In addition, for that particular subcritical condition, the maximum change in dark core length was observed to coincide with the pressure antinode of the acoustic field, while the minimum change occurred near the pressure node.

Similar observations could not be made for the near-critical pressure case due to smaller relative pressure perturbations. Comparing the subcritical condition at MR = 4.2 and near-critical condition at MR = 2, the difference between the maximum and minimum axial dark core lengths for the subcritical condition was 55% larger than the difference between the maximum and minimum axial dark core lengths for the near-critical condition. This difference was 28% larger when using the curved dark core length definition. In addition, it was confirmed that, for subcritical conditions and acoustic fields with pressure perturbations $\Delta p/p$ as high as 3%, the range of momentum flux ratios that show the greatest impact on dark core length lies between MR = 1 and MR = 5. Further investigation of the effects of transverse acoustic fields for near-critical and supercritical conditions will be performed in future studies.

Acknowledgements

The authors would like to thank Mr. Randy Harvey and Lt. Jeffrey Graham for their important contributions running and maintaining the facility. This work is sponsored by AFOSR under Mitat Birkan, program manager.

References

1. Hulka, J., Hutt, J. J., "Instability Phenomena in Liquid Oxygen/Hydrogen Propellant Rocket Engines," Chapter 2, *Liquid Rocket Engine Combustion Instability*, AIAA Progress in Astronautics and Aeronautics Series, Vol. 169, Yang, V., Anderson W. E., editors, 1995,
2. Marshall, W., Pal, S., Woodward, R., Santoro, R. J., Smith, R., Xia, G., Sankaran, V., Merkle, C. L., "Experimental and Computational Investigation of Combustor Acoustics and Instabilities, Part II: Transverse Modes," AIAA-2006-0538
3. Richecoeur, F., Scouflaire, P., Ducruix, S., Candel, S., "High-Frequency Transverse Acoustic Coupling in a Multiple-Injector Cryogenic Combustor" Journal of Propulsion and Power. Vol. 22, No. 4, July-August 2006. pp. 790-799.
4. Leyva, I. A., Chehroudi, B., Talley, D., "Dark-core analysis of Coaxial Injectors at Sub-, Near-, and Supercritical Conditions in a Transverse Acoustic Field", *54th JANNAF Meeting*, Denver, CO, May 14-18, 2007.
5. Leyva, I. A., Chehroudi, B., Talley, D., "Dark-core analysis of Coaxial Injectors at Sub-, Near-, and Supercritical Conditions in a Transverse Acoustic Field", *AIAA-2007-5456*
6. Leyva, I. A., Rodriguez, J. I., Chehroudi, B., Talley, D., "Preliminary Results on Coaxial Jets Spread Angles and the Effects of Variable Phase Transverse Acoustic Fields", AIAA-2008-0950
7. Oschwald, M., Smith, J. J., Branam, R., Hussong, J., Schik, A., Chehroudi, B., Talley, D., "Injection of Fluids into Supercritical Environments", *Combustion Science and Technology*, Vol. 178, No. 1-3, 2006, pp. 49-100.
8. REFPROP, Reference Fluid Thermodynamic and Transport Properties, Software Package, Ver. 7.0, NIST, U.S. Department of Commerce, Gaithersburg, MD, 2002.
9. Thermophysical Properties of Fluid Systems, http://webbook.nist.gov/chemistry/fluid, NIST, U.S. Department of Commerce, 2005.
10. Otsu, N., "A threshold selection method from gray-level histograms", IEEE transactions on Systems, Man, and Cybernetics, Vol. 9, No. 1, 1979, pp. 62-66.

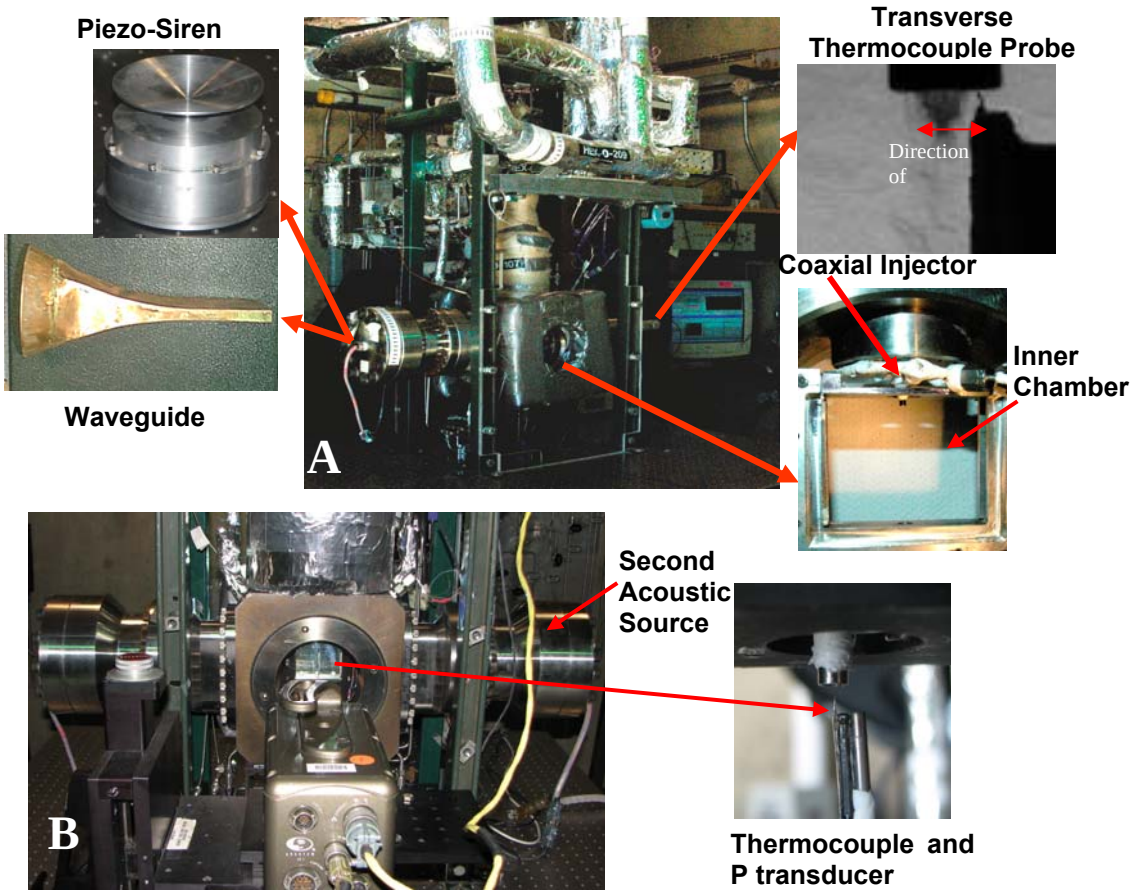

Figure 1. Air Force Research Laboratory's Cryogenic Supercritical Flow Facility, EC-4, at Edwards AFB. The picture labeled "A" shows the facility with only one acoustic source and a transverse thermocouple. Configuration "B" shows two acoustic sources, one at each side of the main test section, where the inner chamber shown is located. A thermocouple and a miniature pressure transducer are introduced from the bottom to measure the temperature of the inner and outer jets and also obtain pressure data to characterize the acoustic field.

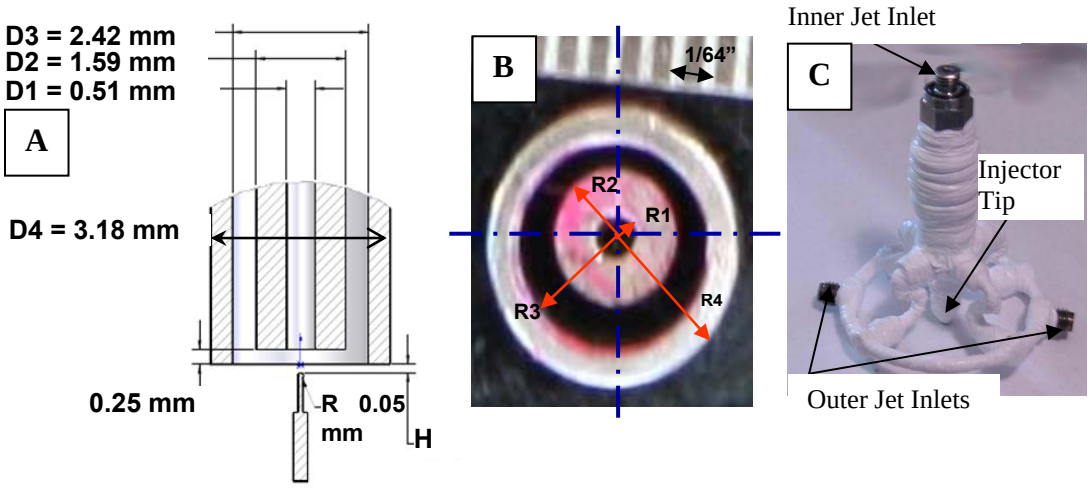

Figure 2. Coaxial injector overview. "A" shows the dimension of the different elements at the tip of the injector. "B" is an actual photograph of the injector tip looking upstream. "C" pictures the injector in its entirety.

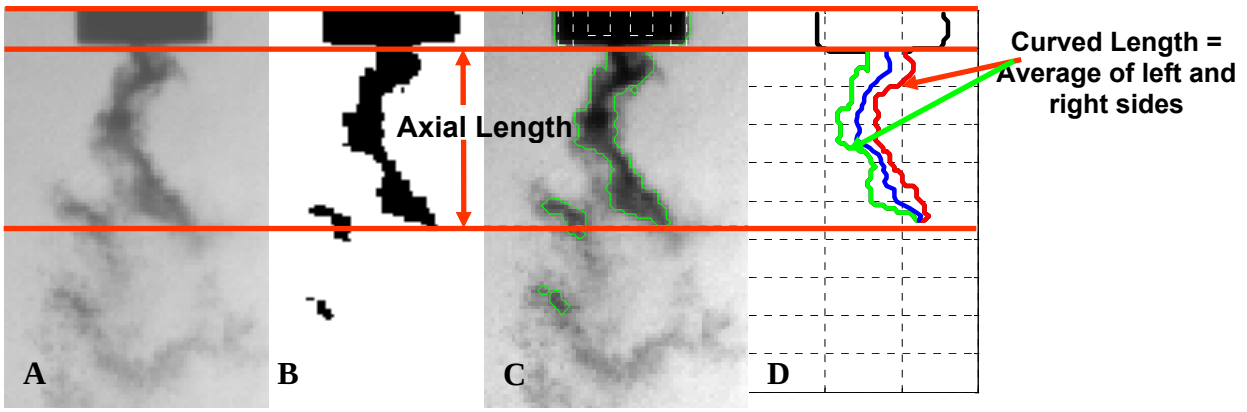

Figure 3. Measuring the dark core length. A. Original image. B. Black and white image after thresholding. C. Contour used to define the axial length. D. Schematic of how the curved length is computed.

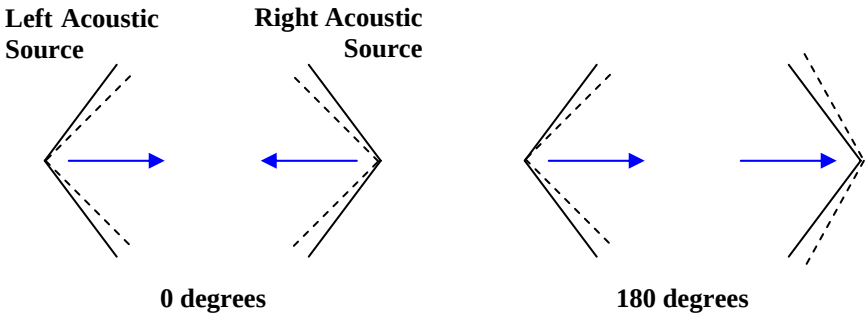

Figure 4. Simplified diagram of the behavior of the two acoustic sources at a 0° and 180° phase angle difference between them.

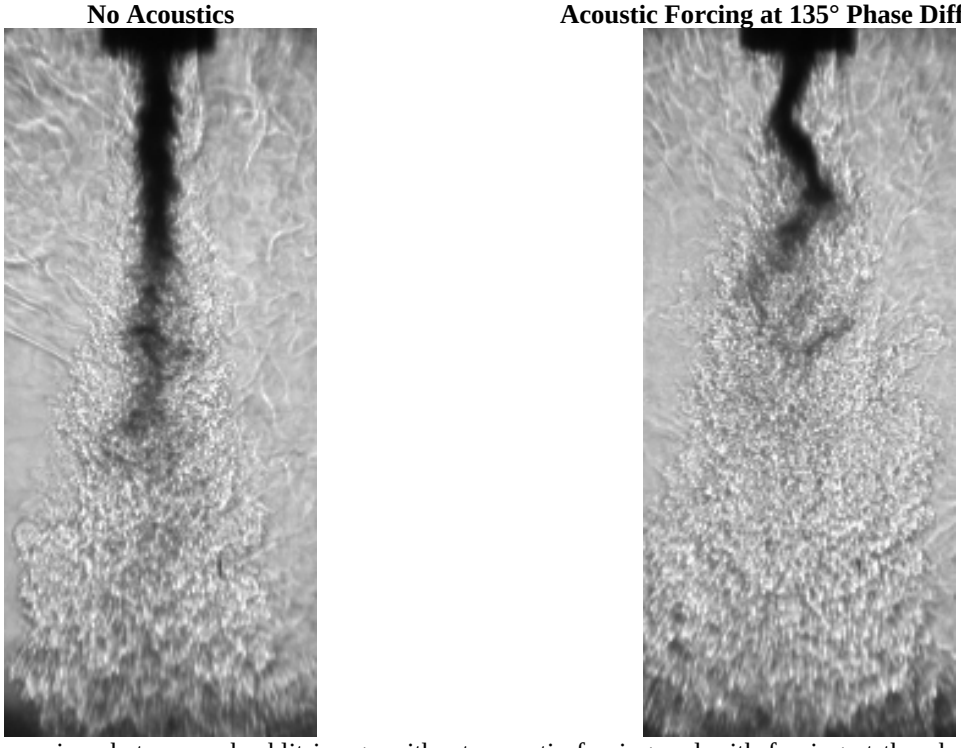

Figure 5. Comparison between a backlit image without acoustic forcing and with forcing at the phase difference (135°) with the maximum effect on dark core length for the subcritical case with MR = 4.2 and P = 1.51 MPa.

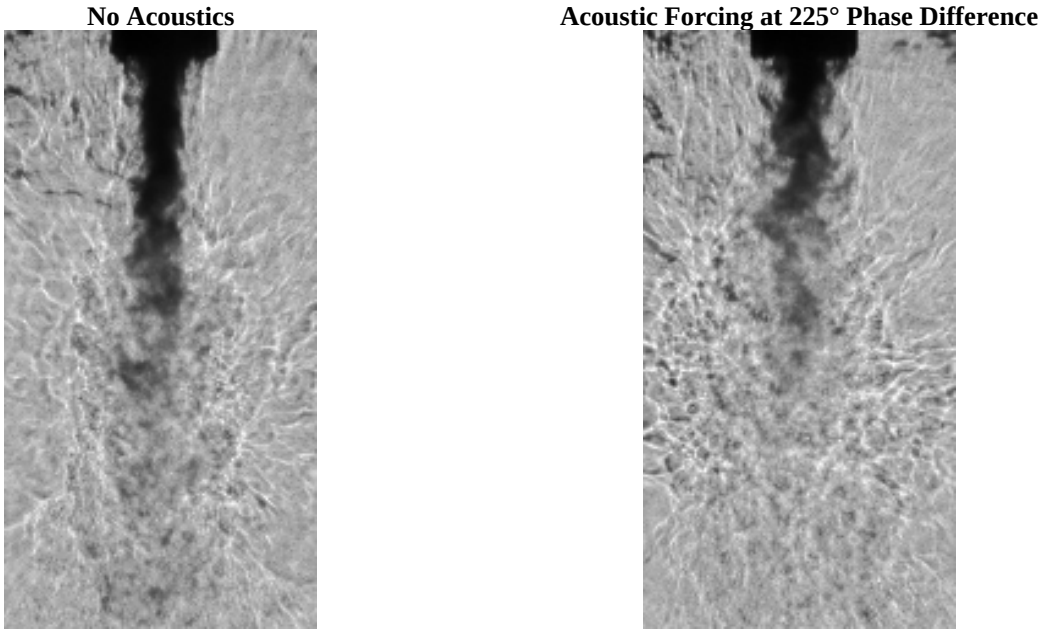

Figure 6. Comparison between a backlit image without acoustic forcing and with forcing at the phase difference (225°) with the maximum effect on dark core length for the near-critical case with MR = 2 and P = 3.55 MPa.

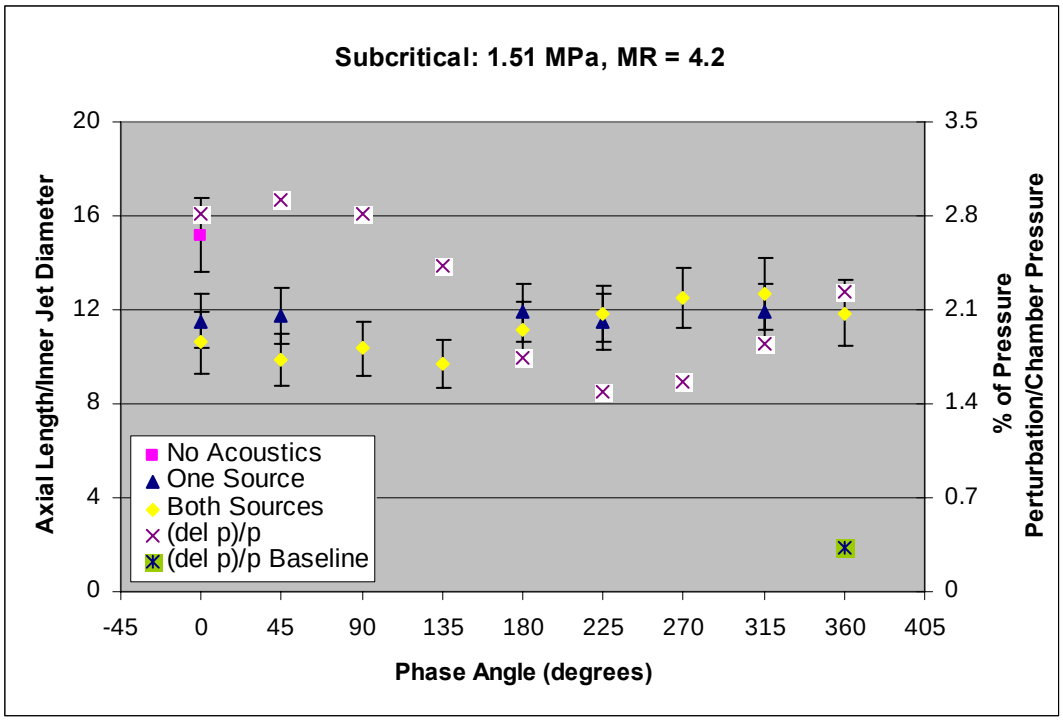

Figure 7. Graph of the axial length normalized by the inner jet diameter for MR = 4.2 at the subcritical pressure of 1.51 MPa. The peak-to-peak pressure perturbation as a percentage of the chamber pressure is also plotted on a secondary axis to show the relationship between the strength of the acoustic field and its impact on dark core length.

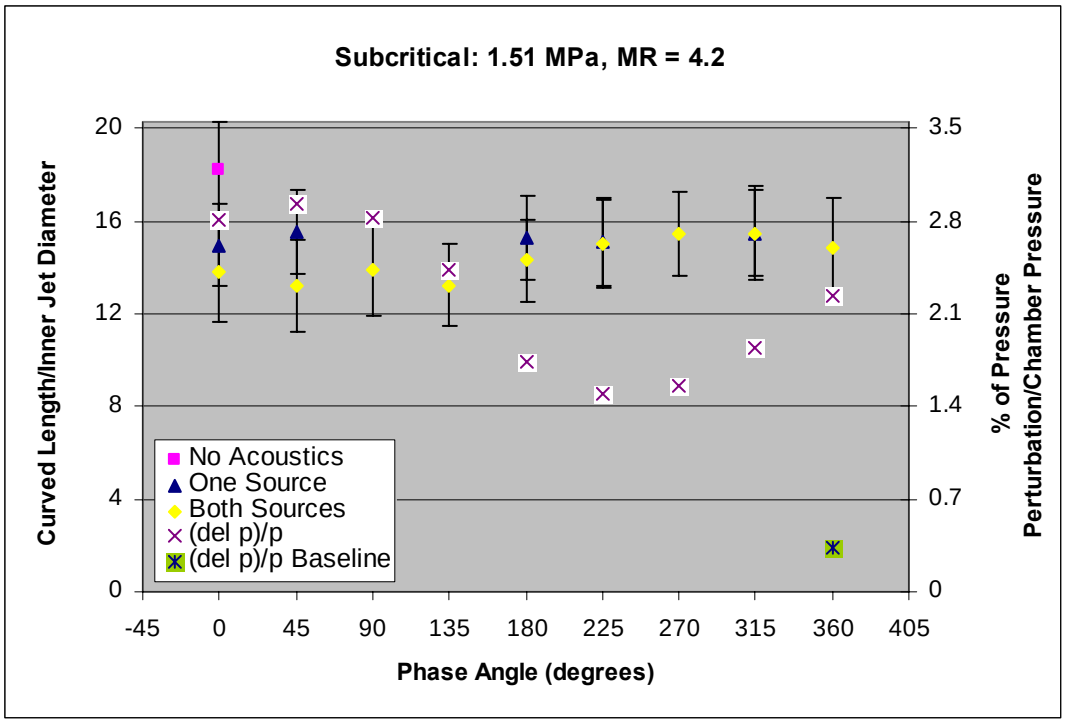

Figure 8. Graph of the total or curved length normalized by the inner jet diameter for MR = 4.2 at the subcritical pressure of 1.51 MPa. The peak-to-peak pressure perturbation as a percentage of the chamber pressure is also plotted on a secondary axis.

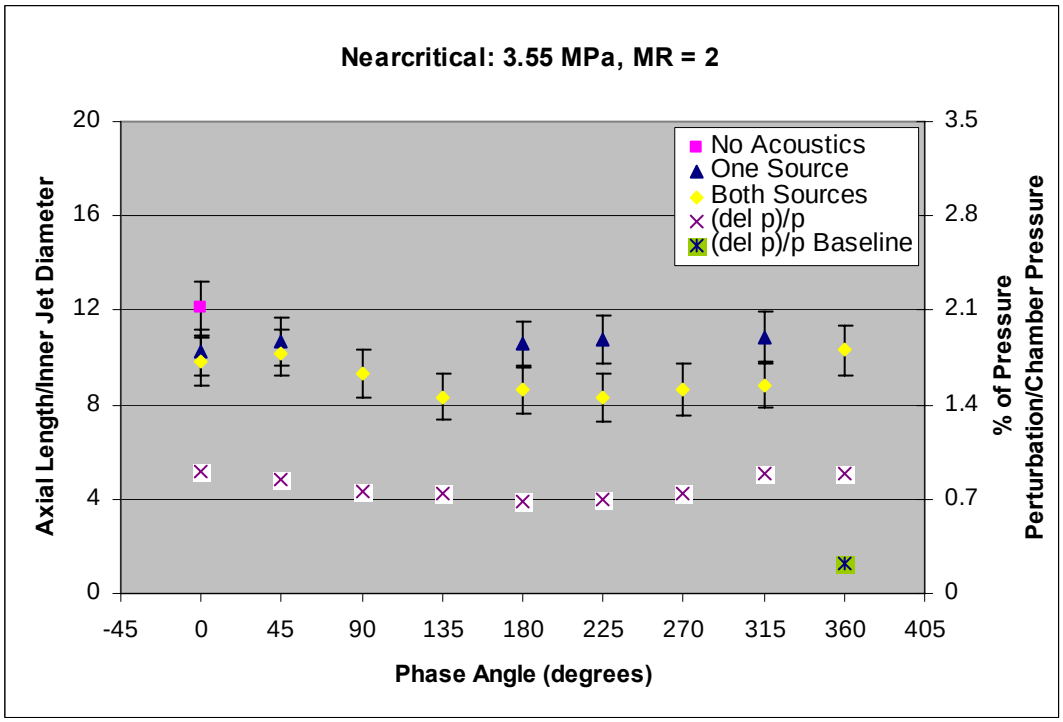

Figure 9. Graph of the axial length normalized by the inner jet diameter for MR = 2 at the near-critical pressure of 3.55 MPa. The peak-to-peak pressure perturbation as a percentage of the chamber pressure is also plotted on a secondary axis to show the relationship between the strength of the acoustic field and its impact on dark core length.

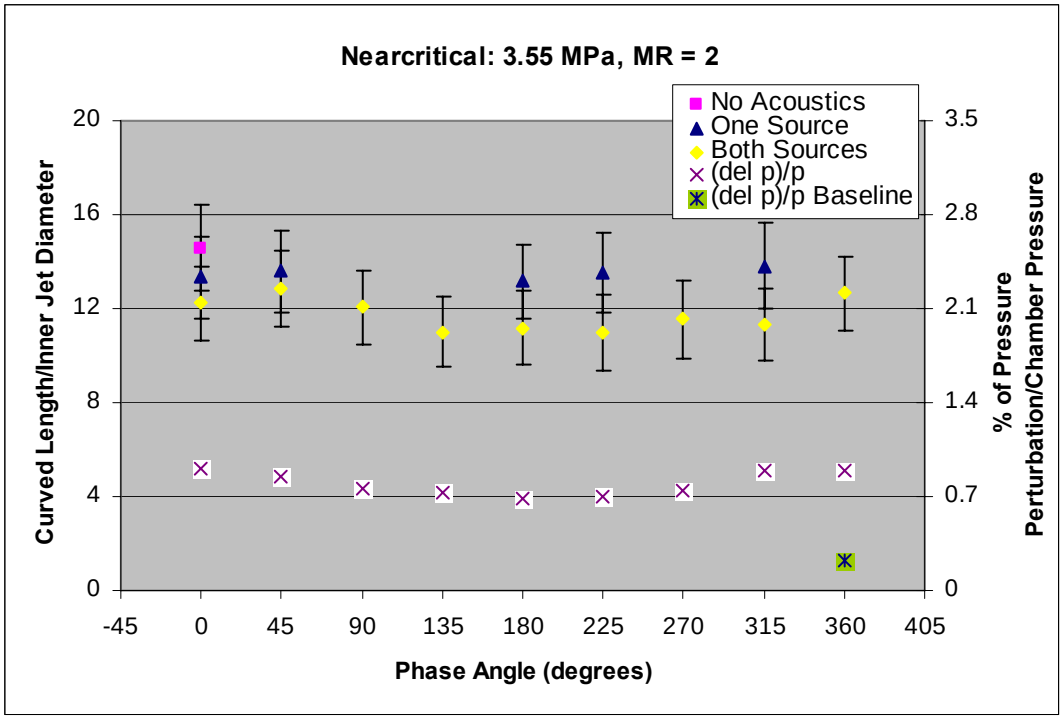

Figure 10. Graph of the total or curved length normalized by the inner jet diameter for MR = 2 at the near-critical pressure of 3.55 MPa. The peak-to-peak pressure perturbation as a percentage of the chamber pressure is also plotted on a secondary axis.

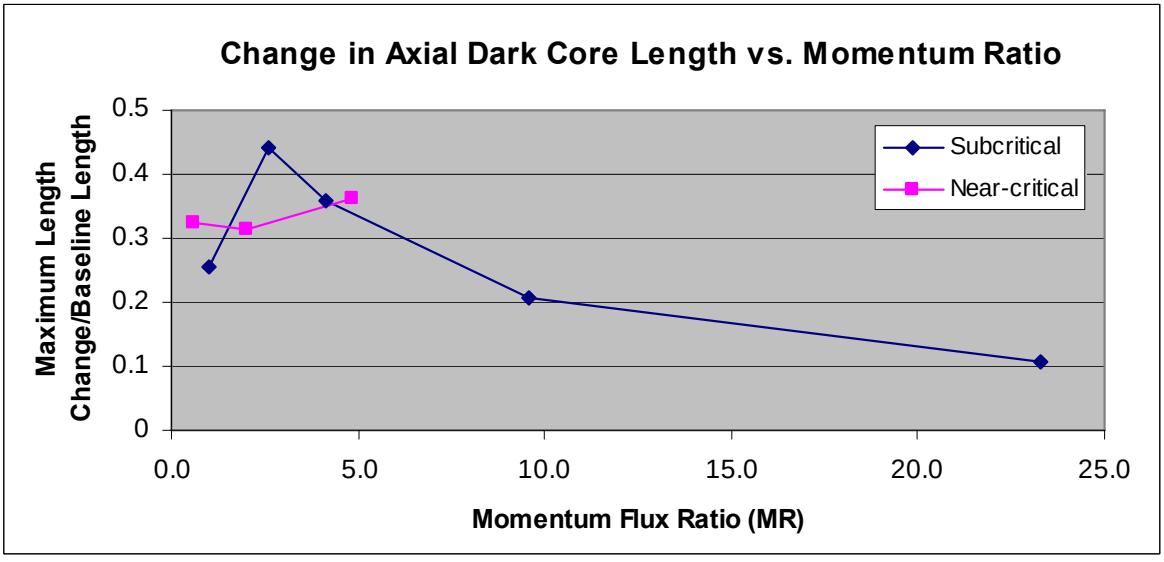

Figure 11. Plot of the maximum axial dark core length change normalized by the axial baseline length observed at each momentum flux ratio.

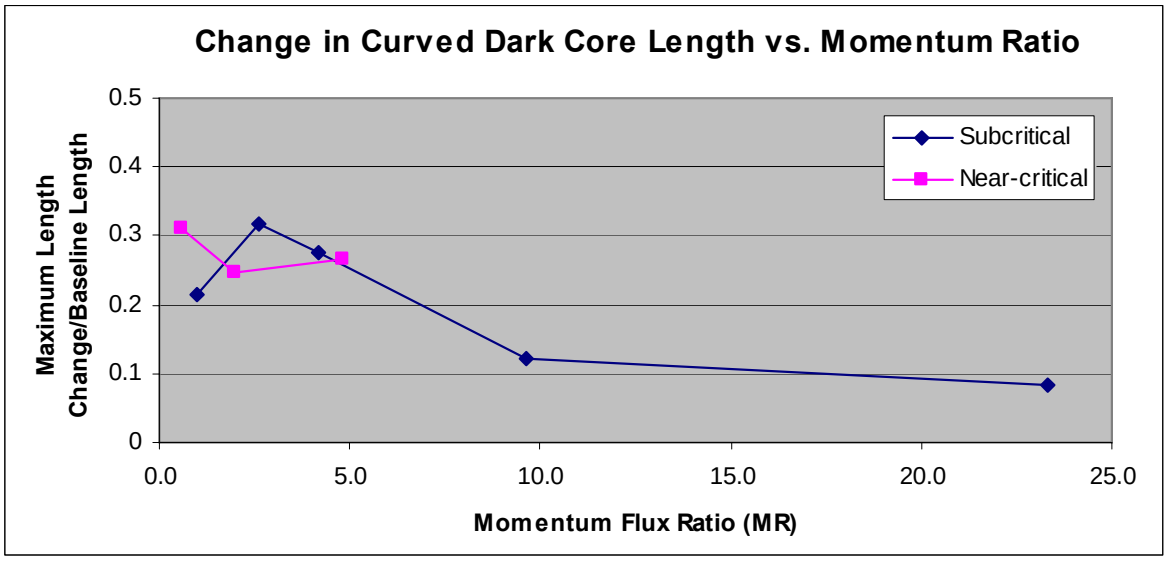

Figure 12. Plot of the maximum curved dark core length change normalized by the curved baseline length observed at each momentum flux ratio.

	$T_{chamber}$ (K)	$\rho_{chamber}$ (kg/m^3)	$P_{chamber}$ (MPa)	T_{outer} (K)	$\dot{m}_{outer}$ (mg/s)	ρ_{outer} (kg/m^3)	u_{outer} (m/s)	T_{inner} (K)	$\dot{m}_{inner}$ (mg/s)	ρ_{inner} (kg/m^3)	u_{inner} (m/s)	VR	MR
SUB													
case1	231	22.2	1.50	183	790	28.8	11	109	283	630	2.2	4.8	1.0
case2	226	21.9	1.45	183	1230	27.8	16.9	109	284	630	2.2	7.6	2.6
case3	226	22.9	1.51	185	1560	28.7	20.9	109	279	630	2.2	9.5	4.2
case4	210	24.9	1.50	182	2400	29.3	31.3	109	279	630	2.2	14	9.6
case5	216	24.1	1.50	191	3640	27.7	50.3	109	279	630	2.2	23	23
NEAR													
case1	223	56.6	3.58	180	1060	75	5.4	123	290	520	2.8	2.0	0.56
case2	223	56	3.55	184	2170	72	12	127	294	400	4	3	2
case3	219	57.6	3.56	194	3080	67	18	125	289	480	3.0	5.9	4.9

Table 1. Summary of the fluid properties and flow conditions for the different cases presented in this study.